Experimental Study of Bit Error Rate of Free Space Optics Communications in Laboratory Controlled Turbulence

H. Le-Minh[*], Z. Ghassemlooy[*], M. Ijaz[*], S. Rajbhandari[*], O. Adebanjo[*], S. Ansari[*] and E. Leitgeb[**]

***Abstract*—This paper reports experimental results for the performance of an free space optical (FSO) communication link employing different modulation schemes under the influence of the atmospheric scintillation. A dedicated experimental atmospheric simulation chamber has been developed where weak and medium turbulence can be generated and its effect on the FSO link is investigated. The experimental data obtained is compared to the theoretical prediction. The paper also shows that the effect on the data transmission performance depends on the position of turbulence source positioned within the chamber.**

***Index Terms*—Free space optics, turbulence, modulation schemes**

I. Introduction

OPTICAL wireless (OW) or FSO communications offers huge capacity for data transmission over medium range distance. FSO links with a direct light of sight configuration offer numerous advantages when compared to the conventional wired and radio frequency (RF) wireless communications. It has a wide unlicensed frequency spectrum, and is capable of transmitting data in excess of 100 Gbit/s when employing wavelength division multiplexing scheme [1]. FSO links also consume relatively low power (meeting the eye safety requirement particularly when operating at 1550 nm wavelength), offer security as well as less susceptibility to the electromagnetic interference [2, 3]. However, FSO systems suffer from substantial optical signal losses due to the atmospheric conditions. The loss is mainly due to the atmospheric absorption, scattering and temperature dependent scintillations [4]. Fog is the major problem with the FSO links. In the moderate continental fog, propagation attenuation can be as high as 130 dB/km reaching 480 dB/km in dense maritime fog condition. In a cloudy condition, the optical loss could be much higher than 50 dB/km. Rain drop could also attenuate the transmitted signal by about 20-30 dB/km at a rain rate of 150 mm/h [4], whereas attenuation due to snow could be greater than 45 dB/km [5].

Apart from the attenuation, the atmospheric scintillation also impairs the FSO link performance. Scintillation is caused by the atmospheric temperature inhomogeneity. In the clear weather condition, theoretical and experimental studies have shown that scintillation could severely degrade the reliability and connectivity of FSO links [6, 7]. As the random changes in the temperature and pressure of the atmosphere create the random variation of the refractive index along the beam transmission path, directions of optical beam could be altered, thus resulting in fluctuation of the received optical signal leading to reduced signal intensity. Theoretical modeling and study of the scintillation effect, one of the most important adverse channel effects, as well as the possible solutions have been addressed by a number of researchers over the last few years.

In practice, however, it is very challenging to measure the effect of the atmospheric turbulence under diverse conditions. This is mainly due to the long waiting time to observe and experience reoccurrence of different atmospheric events. Because of this reason for the first time we have developed a dedicated laboratory atmospheric chamber where it makes possible to create fog, smoke, turbulence, wind etc. and observe and investigates their effects on the transmitted optical beam under a controlled environment.

In this paper we report the experimental study of the temperature induced turbulence effect on the FSO link performance for the on-off keying (OOK) data format, a widely used data format in commercial FSO links. The paper also shows the dependence of the data transmission performance against the turbulence source position along the link. The paper is organized as follows: theoretical model of turbulence is outlined in Section 2. In Section 3 the laboratory atmospheric chamber as well as the experimental setup to investigate the turbulence impact on the optical beam are introduced and explained. Experiment results and analysis are discussed in Section 4. The conclusions and future works are presented in the final Section.

II. Turbulence Model

Atmospheric turbulence results from thermal gradients within the optical path caused by the variation in air temperature and density. Refractive index is highly dependent

This research work is carried out under the EU-COST ACTION IC0802 project.

The authors (*) are with Optical Communications Research Group, School of Computing, Engineering and Information Sciences, Northumbria University (phone: +441912274902; e-mail: fary@ieee.org).

The author (**) is with Institute of Broadband Communications, TU Graz, Austria (e-mail: erich.leitgeb@TUGraz.at).

on the small scale temperature fluctuations in air defined by $n(R,t) = n_o + n_1(R,t)$, where n_o is mean index of refraction ($n_o = 1$) and $n_1(\boldsymbol{R},t)$ is the random deviation of index from its mean value. $\boldsymbol{R}$ is the vector position in three dimension and t is the time. The most commonly reported model for describing the atmospheric turbulence is the log-model model [8, 9]. This is a well-known modeling approach and has been adopted in many calculations for the turbulence channel. As the light propagates through a large number of elements in the atmosphere channel, each induces independently random scattering and phase delay to the optical beam, the distribution of log-amplitude fluctuation is Gaussian. Therefore the power density function (pdf) of the received irradiance I due to the turbulence is derived as [9, 10]:

$$p(I) = \frac{1}{\sqrt{2\pi\sigma_I^2}}\frac{1}{I} exp\left\{-\frac{\left(ln\left(I/I_0\right)+\sigma_I^2/2\right)^2}{2\sigma_I^2}\right\}, \qquad (1)$$

where I_0 is the irradiance when there is no turbulence in the channel. σ_I^2 is log irradiance variance and it is considered as the Rytov parameter.

Figure 1 shows the log-normal pdf plotted for different value of irradiance variance values. As σ_I^2 increases, the distribution spreads its long tail toward the infinity, whereas the received optical signal intensity concentrates below the normalized I_0 due to received signal fading. For a low value of σ_I^2 the distribution is close to the Gaussian.

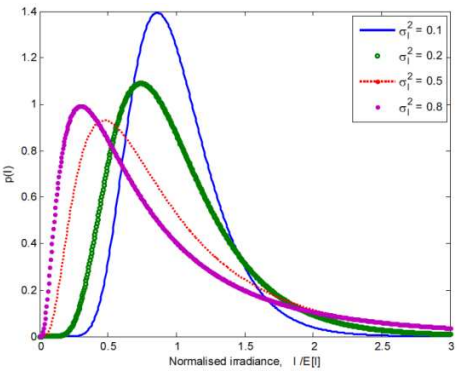

Figure 1. Normalized log-normal pdf for a range of irradiance variance

The log-normal model is valid for the weak atmospheric turbulence [11, 12]. For a strong turbulence multiple scattering effects must be considered, which is not included in (1), therefore improved model should be used [13]. Table I relates the turbulence strength with the Rytov parameter. Here we carry out experimental measurement for the weak and medium turbulence conditions.

TABLE I
TURBULENCE CONDITIONS

Turbulence	Rytov parameter
Weak	$\sigma_I^2 < 0.3$
Medium	$\sigma_I^2 \approx 1$
Strong	$\sigma_I^2 >> 1$

III. EXPERIMENT SETUP FOR TURBULENCE CHANNEL

The experimental line-of-sight FSO link for data transmission through the turbulence channel is shown in Figure 2(a).

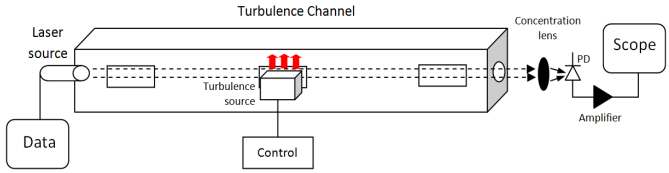

(a)

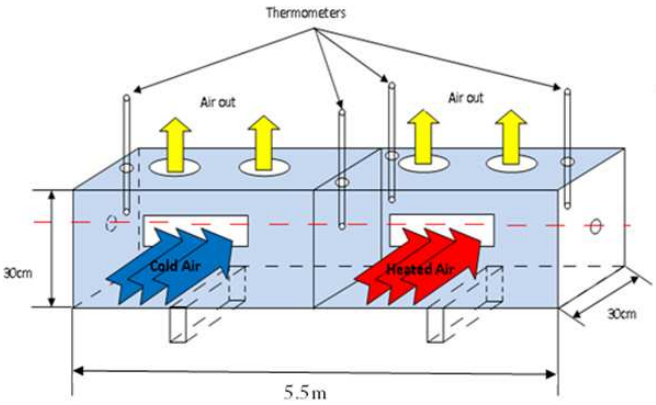

(b)

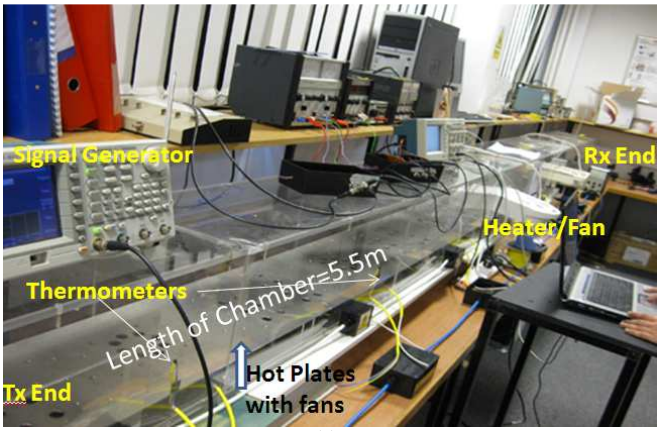

(c)

Figure 2. (a) Block diagram of experiment setup, (b) the laboratory turbulence chamber which are excited by hot and cool air and (c) the chamber and FSO link setup in the laboratory

A narrow divergence beam laser is used as the FSO transmitter. The emitted beam intensity is modulated by a data source which can generate different modulation data formats. To ensure the linearity of the system, the laser is properly biased and modulated.

The laboratory atmospherics channel is a closed glass chamber with dimension of 550×30×30 cm^3 as depicted in Figure 2(b) and (c). The chamber has multiple compartments (seven in total for this experiment), each has a vent to allow air to circulate into and out of the channel. The temperature

and wind velocity conditions in the chamber are controlled as necessary to mimic the atmospheric condition as far as possible. In this chamber, there are two approaches that could be used to create the turbulence effect.

a) Heater and fans are used to blow hot and cold air in the direction perpendicular to signal propagation to generate the variation in temperature and wind speed (see Figure 2(b)). The cold air is at room temperature (20 - 25 °C) and hot air temperature is in a range of 20 to 80 °C. Using a series of air vents, additional temperature control is achieved thus ensuring a constant temperature gradient between the source and the detector.
b) Each compartment has a powerful internal heating source inside the chamber and a fan attached to its vent so that a very strong turbulence effect can be generated.

In this paper we adopt the design (a) to experimentally investigate the weak and medium turbulence as the theoretical model given in (1) is not valid for the strong turbulence.

As the optical beam propagates through the chamber, it experiences different atmospheric turbulence before being collected at the receiver. The receiver front-end consists of an optical concentration lens and a PIN photodetector. The equivalent photocurrent at the output of the photodetector is amplified using a trans-impedance amplifier IC circuit and the recovered data is used to measure the bit error rate (BER) performance. The parameters for the designed chamber is given in Table II

TABLE II
MAIN PARAMETERS OF TURBULENCE CHAMBER

Parameters	Value
Dimension	550×30×30 cm^3
Temperature range	20 - 80 °C
Wind speed	4 - 5 m/s

The level of turbulence strength is controlled by placing the same heating source near and far away from the FSO transmitter. Ray tracing diagram in Figure 3 illustrates this concept. The optical beams shown in both Figure 3(a) and (b) could approximately experience the same degree of bending due to the same level-controlled turbulence source is used, however due to geometry configuration less power will be collected at the receiver shown in Figure 3(a) than in Figure 3(b).

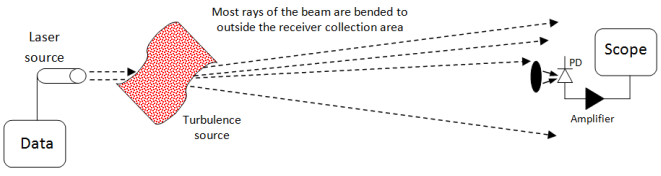

(a)

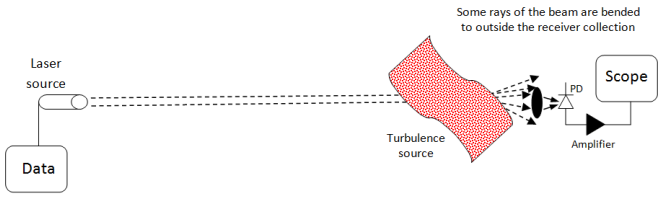

(b)

Figure 3. Sketch of diverted beams due to turbulence source positioned (a) near the transmitter and (b) near the receiver

IV. RESULTS AND DISCUSSIONS

The purpose of this demonstration is to investigate the performance of the BER of an FSO link under the effect of atmospheric turbulence. For valid comparisons, the measurements carried out in the laboratory environment are taken in similar environmental conditions as far as possible. A pseudorandom binary sequence (PRBS) of $2^{13} - 1$ bit length directly modulates the laser source whose emitted beam propagates through the chamber. Data packets with length of (~ 600 - 1200 bytes) are of typical in the Gigabit Ethernet (GbE) data networks. Further details of the setup and parameters used for the demonstration are shown in Table III.

TABLE III
PARAMETERS OF FSO COMMUNICATIONS LINK DEMONSTRATION

Parameter		Value
Data source	PRBS length	$2^{13} - 1$
	Format	NRZ / RZ
	Modulation voltage	LVDS (400 mV_{pp})
Laser diode	Peak wavelength	830 nm
	Maximum optical power	10mW
	Class	IIIb
	Beam size at aperture	5mm × 2 mm
	Beam divergence	5 mrad
	Modulation bandwidth	75 MHz
Photodetector	Wavelength at maximum sensitivity	900 nm
	Spectral range of sensitivity	750 - 1100 nm
	Active area	1 mm^2
	Half angle field of view	± 75 Deg
	Spectral sensitivity	0.59 A/W
	Rise and fall time	5 ns
	Reversed bias voltage	40 V
Lens	Diameter	25 mm
	Focal length	200 mm
Receiver	Transamplifier (IC)	AD8015
	Bandwidth	240 MHz
	Transimpedance amplifier gain	15 kΩ

Turbulence is generated inside the chamber by pumping hot air through either one of vents near transmitter or in the middle of chamber or near the receiver. Table IV shows the measured values of σ_I^2 at these positions. The shot noise variance is already excluded from these reported σ_I^2 in the Table. Note that by using the same turbulence source and varying its position along the link, we could generate different levels of turbulence (i.e. σ_I^2) according to the concept sketched in Figure 3. The concept is also valid for the actual outdoor

FSO systems.

For the measured σ_I^2 of 0.8 and 0.6, turbulence generated in the chamber could be equivalently considered as medium turbulence for outdoor environment. Histogram of bit '1' of the received signal induced by the medium turbulence is obtained and plotted in Figure 4. The distribution of received signal is Gaussian when there is no turbulence effect on the channel (see Figure 4(a)), as the Gaussian-distributed shot noise (due to ambient noise) is dominant. However the received signal pdf profile is changed to the log-normal when turbulence is introduced with the channel.

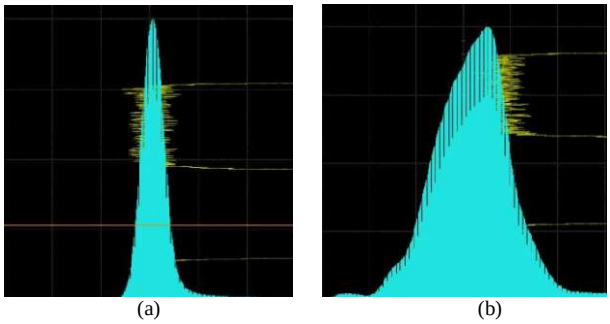

(a) (b)

Figure 4. Histogram of '1'-bit received signal in case of (a) no turbulence and (b) medium turbulence with $\boldsymbol{\sigma_I^2}$ = 0.8

TABLE IV
MEASUREMENT RESULTS OF TURBULENCE STRENGTH
INSIDE THE CHAMBER CHANNEL

Turbulence position	**Near transmitter**	**Middle of the chamber**	**Near receiver**
Rytov variance	σ_I^2 = 0.8	σ_I^2 = 0.6	σ_I^2 = 0.23
Turbulence strength	Medium	Medium	Weak

As the result of turbulence, the eye opening of received signal eye diagram is reduced due to considerable level of signal intensity fluctuation observed in Figure 4(b). Measured eye diagrams for the non-return to zero (NRZ) data format at different data rates (20 and 155 Mbit/s) are depicted in Figure 5. The modulation input voltage is LVDS (400 mV_{pp}). It is noticed that the top (bit '1') and base (bit '0') levels of received signals are varied at much wider margin when turbulence is introduced. This will result in the reduction of the measured *Q* factor and hence the BER performance.

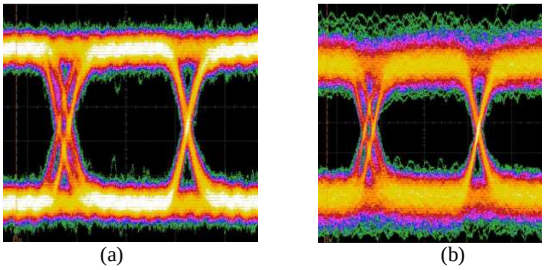

(a) (b)

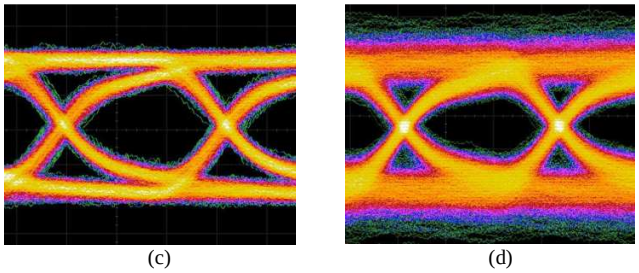

(c) (d)

Figure 5. The measured eye diagram of received NRZ signal in the condition of (a) no turbulence, data rate of 20 Mbit/s, (b) weak-medium turbulence with $\boldsymbol{\sigma_I^2}$ = 0.8, data rate of 20 Mbit/s, and (c) no turbulence, data rate of 155 Mbit/s, (d) weak-medium turbulence with $\boldsymbol{\sigma_I^2}$ = 0.8, data rate of 155 Mbit/s

Figure 6 plots the eye diagram of RZ signal in comparison to the NRZ signal at a data rate of 20 Mbit/s. The difference between the experimental conditions for obtaining the NRZ eye diagram in Figure 6(c) and for the plots shown in Figure 5 is the modulation level. In Figure 6(c) the NRZ modulation signal intensity is 200 mV, which is selected to ensure the average transmit energy in both NRZ and RZ format is the same value as we apply LVDS RZ signal to modulate the laser. From the eye diagrams the measured *Q* factor for RZ signaling is higher than NRZ signaling; therefore the RZ modulation format would be less susceptible to the turbulence than the NRZ case.

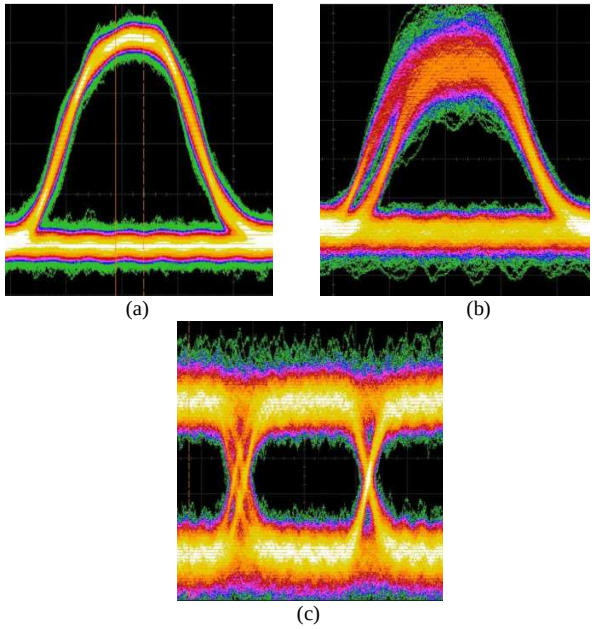

(a) (b)

(c)

Figure 6. The measured eye diagram of received 20 Mbit/s RZ signal in the condition of (a) no turbulence, (b) weak-medium turbulence with $\boldsymbol{\sigma_I^2}$ = 0.8 and (c) NRZ signal with $\boldsymbol{\sigma_I^2}$ = 0.8. Both NRZ and RZ signal have the same average transmit energy

In this demonstration the emphasis is on the turbulence effect therefore we have selected a range of two data speeds to observe the different outcomes of data transmission performance. A data rate of 20 Mbit/s is well within the optoelectronic bandwidth of the given FSO link (see a clear eye diagram in Figure 5(a)), therefore we can clearly observe

the penalty induced by turbulence. When no turbulence within the channel, $\sigma_I^2 = 0$, Q is up to 15, see Figure 7(a). However its value is dropped considerably to ~5 when weak-medium turbulence ($\sigma_I^2 = 0.8$) is introduced. On the other hand data transmission at a rate of 155 Mbit/s (about the maximum rate of the FSO system) suffers less Q penalty due to the turbulence-free received signal being already distorted. Figure 7(b) shows the BER plots corresponding to each data rate values. Note that BER values below 10^{-12} are truncated to that level.

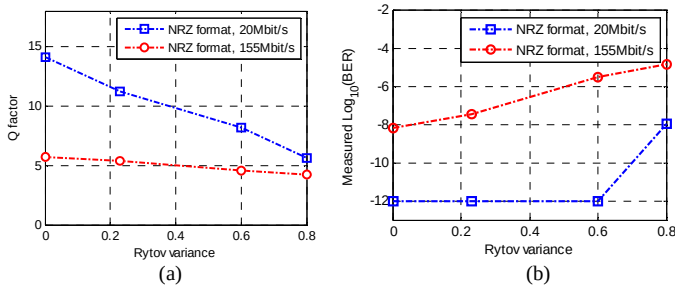

(a) (b)

Figure 7. (a) Measured Q values and (b) BER performance against a range of Rytov variance (or turbulence strength) for NRZ signaling at different speed (modulation voltage is 400mW)

Figure 8 shows performance of RZ and NRZ signaling in the present of turbulence. It is shown that RZ outperforms NRZ in the weak turbulence scenario, however the performance of both data formats are almost the same in the medium turbulence region. This could be explained by the fact that turbulence not only induces amplitude fluctuation but it could cause timing jitter. Therefore RZ signaling is more susceptible to jitter in the case of medium and strong turbulence, whereas NRZ, with wider bit duration, experiences less effect (see Figure 6).

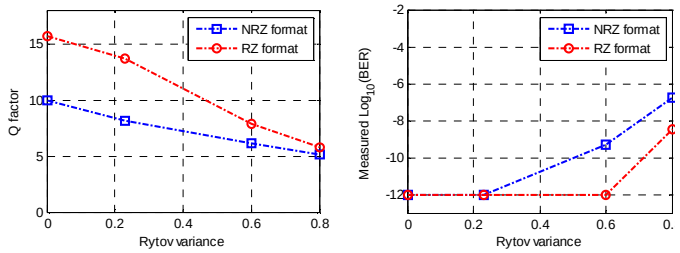

(a) (b)

Figure 8. (a) Measured Q values and (b) BER performance against a range of Rytov variance for NRZ and RZ signaling at 20 Mbit/s (modulation voltage is 400mW for RZ and 200mV for NRZ)

V. CONCLUSIONS

The paper presented a dedicated laboratory atmospheric chamber where the effect of the temperature induced turbulence on the FSO link performance was investigated. Methods to generate and control turbulence were discussed and practically demonstrated. The obtained data showed that the medium turbulence can severely affect the link performance. The turbulence effect is also dependent on the data format being adopted to directly modulate the laser source. The RZ signaling format offers improved resistance to the turbulence than the NRZ due to its higher peak voltage albeit the need for higher bandwidth requirement and more susceptibility to the jitter noise.

Work to investigate strong turbulence scenario is going on and would be published in due course.

REFERENCES

[1] N. Cvijetic, Q. Dayou, Y. Jianjun, H. Yue-Kai, and W. Ting, "100 Gb/s per-channel free-space optical transmission with coherent detection and MIMO processing," in *ECOC 2009*, Vienna, Austria, 2009, pp. 1-2.

[2] Z. Xiaoming and J. M. Kahn, "Free-space optical communication through atmospheric turbulence channels," *IEEE Transactions on Communications*, vol. 50, pp. 1293-1300, 2002.

[3] W. O. Popoola and Z. Ghassemlooy, "BPSK subcarrier intensity modulated free-space optical communications in atmospheric turbulence," *IEEE Journal of Lightwave Technology*, vol. 27, pp. 967-973, 2009.

[4] M. A. Naboulsi, H. Sizun, and F. d. Fornel, "Fog attenuation prediction for optical and infrared waves," *Optical Engineering*, vol. 43, pp. 319-329, 2004.

[5] M. S. Awan, L. C. Horwath, S. S. Muhammad, E. Leitgeb, F. Nadeem, and M. S. Khan, "Characterization of fog and snow attenuations for free-space optical propagation," *Journal of Communications*, vol. 4, pp. 533-545, 2009.

[6] W. Gappmair and M. Flohberger, "Error performance of coded FSO links in turbulent atmosphere modeled by gamma-gamma distributions," *IEEE Transactions on Wireless Communications*, vol. 8, pp. 2209-2213, 2009.

[7] T. A. Tsiftsis, H. G. Sandalidis, G. K. Karagiannidis, and M. Uysal, "Optical wireless links with spatial diversity over strong atmospheric turbulence channels," *IEEE Transactions on Wireless Communications*, vol. 8, pp. 951-957, 2009.

[8] S. Karp, R. M. Gagliardi, S. E. Moran, and L. B. Stotts, *Optical Channels: fibers, clouds, water and the atmosphere*. New York: Plenum Press, 1988.

[9] G. R. Osche, *Optical Detection Theory for Laser Applications*. New Jersey: Wiley, 2002.

[10] J. W. Goodman, *Statistical Optics*. New York: John Wiley, 1985.

[11] D. Kedar and S. Arnon, "Urban optical wireless communication networks: the main challenges and possible solutions," *IEEE Communications Magazine*, vol. 42, pp. s2-s7, 2004.

[12] X. Zhu and J. M. Kahn, "Free-space optical communication through atmospheric turbulence channels," *IEEE Transactions on Communications*, vol. 50, pp. 1293-1300, 2002.

[13] M. Uysal, J. T. Li, and M. Yu, "Error rate performance analysis of coded freespace optical links over gamma-gamma atmospheric turbulence channels," *IEEE Transactions on Wireless Communications*, vol. 5, pp. 1229-1233, 2006.